High Temperatures - High Pressures, 1979, volume 11, pages 75-86

Spherical acoustic resonators for temperature and thermophysical property measurements

Michael R Moldover, Meyer Waxman, Martin Greenspan¶
Thermophysics Division, National Bureau of Standards, Washington, DC 20234, USA
Presented at the 6th European Thermophysical Properties Conference, Dubrovnik, 26-30 June 1978

Abstract. A theoretical and experimental study is reported of the advantages and limitations of using the acoustic radial resonances in a spherical cavity to obtain thermophysical property data in dilute gases. The velocity of sound in dilute gases (0·1-0·5 MPa) is now measured with an accuracy of 0·02% and a precision of 0·001%, and a significant increase in accuracy is anticipated. The measurements are at sufficiently low frequencies (3-15 kHz) to be of value in determining thermophysical properties in many polyatomic gases.

1 Introduction

In the recent past, very accurate velocity-of-sound measurements in dilute gases have been used to obtain information on a variety of important thermophysical properties. We mention three examples: (i) the equations of state of methane, helium, and ethylene have been derived (Gammon 1976, 1979; Gammon and Douslin 1976); (ii) the thermodynamic temperature scale has been established in the 4-20 K range (Plumb and Cataland 1966; Cataland and Plumb 1973); and (iii) the gas constant, R, has been redetermined by a measurement of the velocity of sound in argon at the temperature of the triple point of water (Quinn et al 1976). In each of these examples a cylindrical acoustic interferometer was used for the measurement.

The primary purpose of this paper is to suggest that spherical resonators, particularly when used in radial modes, have many practical advantages in comparison with cylindrical interferometers for obtaining thermophysical properties from velocity-of-sound measurements in dilute gases. Perhaps the most important of these are:

(i) The resonance frequencies of the radial modes in a sphere are sensitive to geometrical imperfections in second order, thus for practical purposes only the resonator's volume needs to be known.

(ii) The correction to the measured resonant frequencies resulting from the gas-resonator wall interactions can be an order of magnitude smaller in a spherical resonator than in a cylindrical interferometer.

(iii) The very high Qs of the radial modes in a sphere (2200-6100 in our data) allow the experimenter to choose among many types of transducers and alternative schemes for coupling them to the resonator. We have chosen to place transducers outside the resonator. This choice may be particularly convenient for velocity-of-sound measurements at high temperatures. The resonator can be at a high temperature while the transducers are near ambient temperature.

Our ultimate objective is to develop practical spherical resonators and theoretical models to describe them to a level of accuracy where they can be used for the most demanding applications such as an acoustic determination of the absolute temperature or an acoustic measurement of the gas constant. If this is achieved, it is likely that measurements using spherical resonators will routinely provide useful information about the thermal conductivity and viscosity of gases, in addition to the specific-heat

¶ Present address: 12 Granville Drive, Silver Spring, Md 20901, USA.

and equation-of-state data which are more commonly derived from velocity-of-sound measurements.

In this paper we will report the progress in the development of our theoretical model for spherical resonators and some preliminary experimental results. The latter include a measurement of the velocity of sound in argon near ambient temperature and pressure with an accuracy of about 0·02% and a precision of ±0·001% (standard deviation). We expect that both the accuracy and precision can be improved. We have also measured the first derivative of the dependence of the velocity of sound on pressure in argon. Our preliminary value for this derivative is close to that obtained by Rowlinson and Tildesley (1977) in a review of literature data for argon. Our measurements of the losses in the resonator suggest that, at the current state of development, measurements of the thermal diffusivity with an accuracy of a few percent should be possible.

We will conclude this introductory section by briefly contrasting the design and measurement problems encountered upon using spherical resonators with those encountered with conventional interferometers. In section 2 we will discuss our progress in modeling a spherical resonator. Section 3 is concerned with experimental techniques and section 4 describes our preliminary results.

The sources of systematic error in cylindrical interferometers have been reviewed by Colclough (1973). He concluded that in high-frequency interferometers (i.e. interferometers in which many wavelengths fit within the resonant cavity) a problem of unresolved modes may exist. To interpret the observed resonances accurately, one needs to know the distribution of energy among the various modes that fall within a single resonance. To obtain this knowledge, one would have to know many details of the complex transducer motion, because the transducer which excites the resonant cavity usually comprises one of the end walls of the cylindrical resonator. In low-frequency interferometers this problem does not exist. Every mode is resolved. On the other hand at low frequencies the Kirchhoff–Helmholtz correction to the measured resonance frequencies becomes substantial. This correction, which arises from the interaction of the gas and the interferometer wall, must be measured with care and/or calculated from knowledge of both the thermal and the viscous diffusivities of the gas. In the recent gas-constant measurement in a 3 cm diameter resonator, this correction (in argon at 0·1 MPa, 273 K, and at 5·6 kHz) was typically 0·16% (Quinn et al 1976).

Spherical resonators, as we are using them, correspond to low-frequency fixed-path-length interferometers. Every mode of interest is resolved. Our resonator is 12·7 cm in diameter and has its lowest radial resonance at 3·6 kHz (in argon at 0·1 MPa and 273 K). The correction to this resonance frequency which corresponds to the Kirchhoff–Helmholtz correction is 0·022%. This correction is much smaller than the Kirchhoff–Helmholtz correction for three reasons: (i) viscous damping at the resonator walls does not occur for the radial modes in a sphere (or cylinder); (ii) the surface-to-volume ratio is smaller in a sphere than in any other cavity of the same volume; and (iii) the acoustic energy density is highest in the center of the sphere.

In variable-path interferometers, one end of the cylindrical cavity is moved and the displacement required to achieve successive resonances is measured. Although this procedure may require that somewhat complicated mechanical, thermal, and optical design problems be solved, it does result in an absolute measurement of the wavelength of the standing wave of sound. This wavelength measurement may be independent of the temperature and gas pressure in the interferometer, and is independent of the acoustic properties of the transducer which forms one wall of

the interferometer. Such a displacement measurement is impractical with a spherical resonator. As an alternative, one measures the volume of the spherical cavity and then determines its changes with pressure and temperature in auxiliary experiments. Our preliminary experiments suggest that the study of microwave resonances in the spherical cavity is a practical means for accomplishing this.

The elastic response of the resonator walls may be calculated more accurately for a spherical resonator than for a cylindrical interferometer. The spherical resonator does not have the ends and corners which complicate the analysis of vibrations of a cylinder.

2 Progress in the theoretical modeling of spherical acoustic resonators

In order to predict the behavior of our resonator we have first considered the very simple approximation used by Rayleigh (1894). He calculated the resonance frequencies for a fluid bounded by a perfectly rigid spherical wall. This first approximation neglects effects arising from the temperature wave associated with the sound wave as well as attenuation within the fluid. The most important improvement to Rayleigh's model in the case of radial oscillations in dilute gases comes from the consideration of the temperature wave. We have also considered the much smaller effects on the resonator behavior which result from attenuation within the gas, small departures from a spherical shape, and the elastic response of the resonator walls. In future work we plan to consider the effects of small holes used to bring sound into and out of the resonator. We have not made a detailed study of nonradial acoustic modes in a sphere. Such modes would cause the resonator walls to undergo complex vibrations which we are not prepared to consider at the present time. We will now outline our results to date.

In the first approximation discussed by Rayleigh, the velocity, c, potential obeys a wave equation. When the wave equation is separated in spherical coordinates, the radial dependence of the velocity potential has the form $j_n(\beta r)$ in which j_n are the various spherical Bessel functions ($n = 0, 1, 2, \ldots$) and $\beta = \omega/c$. The condition that the normal velocity vanish at the resonator wall, that is at $r = a$, is

$$\frac{\mathrm{d}j_n(\beta a)}{\mathrm{d}a} = 0 . \tag{1}$$

We denote the successive roots of equation (1) by the integer $\ell = 1, 2, 3, \ldots$. Thus (n, ℓ) denotes the ℓth root of equation (1) for the nth spherical Bessel function. In figure 1 we have indicated the location of the lowest 26 roots of equation (1) as well as the acoustic response of our sphere in air at 23 °C (details of the measurements will be given below). The solutions to equation (1) for which $n = 0$ are purely radial modes. They are indicated with arrows in figure 1. For these modes, equation (1) may be written in the form

$$1 - \beta a \cot(\beta a) = 0 . \tag{2}$$

To include the effects of the temperature changes associated with the sound wave we return to the Navier–Stokes equations and construct solutions which consist of the sum of two terms. Each one has the time dependence $e^{i\omega t}$. The first wave (1-wave) is sound-like. It has a propagation constant with a small real part, α, at the audio acoustic frequencies of interest:

$$\Gamma_1 = \alpha + \frac{i\omega}{c} . \tag{3}$$

The second wave (2-wave) is heat-like and has a propagation constant Γ_2 whose square is purely imaginary:

$$\Gamma_2 = \left(\frac{i\omega}{D_t\gamma^2}\right)^{1/2} ; \tag{4}$$

here D_t is the thermal diffusivity and γ is the specific heat ratio c_p/c_v. If we were interested in vibrations that were not purely radial, we would have to introduce a shear wave at this point. For the radial modes a combination of the sound-like and heat-like waves is chosen such as to satisfy two boundary conditions at the cavity wall: (i) the velocity vanishes, and (ii) the temperature is continuous. The latter condition is essentially equivalent to the condition that the temperature is constant at the wall, because the product $c_p D_t^{1/2}$ for the metal wall is between 10^3 and 10^4 times the product for the gas (c_p is the specific heat at constant pressure). The equation determining the propagation constant, analogous to equation (2), now becomes:

$$1 - \beta a \cot(\beta a) = -\frac{\omega^2 a(\gamma-1)}{c^2}\left(\frac{D_t}{i\omega}\right)^{1/2} = \frac{i-1}{2Q_w}(\beta a)^2 . \tag{5}$$

The right-hand side of equation (5) is small compared to unity and has equal real and imaginary parts. Thus, to a good approximation, the values of β which satisfy (5) differ from the values of β which satisfy (2) by the addition of a small number which has equal real and imaginary parts. From these considerations we find resonant frequencies which are

$$f = f_0\left(1 - \frac{1}{2Q_w}\right) ; \qquad Q_w = \left(\frac{\omega a^2}{2D_t(\gamma-1)^2}\right)^{1/2} , \tag{6}$$

where f_0 are the frequencies when the thermal wave is neglected, and Q_w is the contribution to the Q of the resonances which results from the irreversible nature of the heat flow in the thermal wave near the wall.

The frequency shift proportional to $(2Q_w)^{-1}$ is entirely analogous to the frequency shift which occurs in microwave cavities because of the nonzero resistivity of the cavity walls (Slater 1959). A damped electromagnetic wave pentrates the cavity wall. To the extent that Ohm's law is valid at microwave frequency in the wall, this damped wave has a propagation constant whose square is purely imaginary, in exact analogy with the thermal wave in the acoustic case.

The 'classical' losses in the gas throughout the volume of the cavity make a contribution to the line width similar to that in a plane wave. For a monatomic gas this loss is given by

$$\frac{1}{Q_c} = \frac{2\alpha}{\beta} = \frac{\omega}{c^2}\left(\tfrac{4}{3}D_v + \tfrac{2}{3}D_t\right) . \tag{7}$$

Here D_v is the viscous diffusivity obtained by dividing the viscosity by the density. This contribution to the loss plays a role in the acoustic cavity analogous to the role played by dielectric losses in microwave cavities. In particular it leads to frequency shifts proportional to Q_c^{-2} where the constant of proportionality will depend upon the manner in which the resonance is excited and detected. (For example the excitation might be such that the sound pressure at a point is independent of frequency or, alternatively, that the velocity at some point is independent of frequency.) For the cases we have examined Q_c^{-2} is much less than 10^{-6}; hence this frequency shift may be neglected. On the other hand the classical losses will contribute an easily measured amount to the observed Q of the resonance. Again the analogy with

microwaves holds, and we expect:

$$\frac{1}{Q_{\text{measured}}} = \frac{1}{Q_{\text{c}}} + \frac{1}{Q_{\text{w}}} + \frac{1}{Q_{\text{residual}}} , \tag{8}$$

where the term denoted by Q_{residual} arises from other sources we have not yet considered, such as damping within the cavity wall, radiation of sound, etc.

The walls of laboratory resonators are not perfectly rigid. We have made some preliminary estimates of the effects of the finite mechanical admittance of the walls of our aluminum resonator. These estimates suggest that, under the experimental conditions discussed below, the resonance frequencies will be shifted on the order of 5–9 parts in 10^6 in argon at 0·1 MPa and 0 °C. This shift is proportional to the gas density. The shift becomes very large at frequencies near 20 kHz where the resonator wall itself has a breathing mode.

We have considered the effect of geometrical imperfections on the frequencies of the radial modes. From the adiabatic principle, one may argue that small deformations of the resonator from a perfectly spherical shape will not change the resonance frequencies of the radial modes so long as the volume of the resonator is unchanged. A specific illustration of this idea occurs in the context of nuclear physics (Moszkowski 1955). There, it has been shown that the eigenvalues of the s states of a particle in a spheroidal box are quadratic functions of a parameter which is a measure of small deformations of a sphere into a spheroid while the volume is held constant. On this basis we expect that spherical resonators manufactured to machine shop tolerances will behave very nearly like a perfectly spherical resonator, at least for the radial modes.

We plan to continue our work in modeling the effects of the elastic response of the resonator shell, and in the near future we hope to begin modeling the effects of alternative schemes of exciting and detecting sound within the resonator.

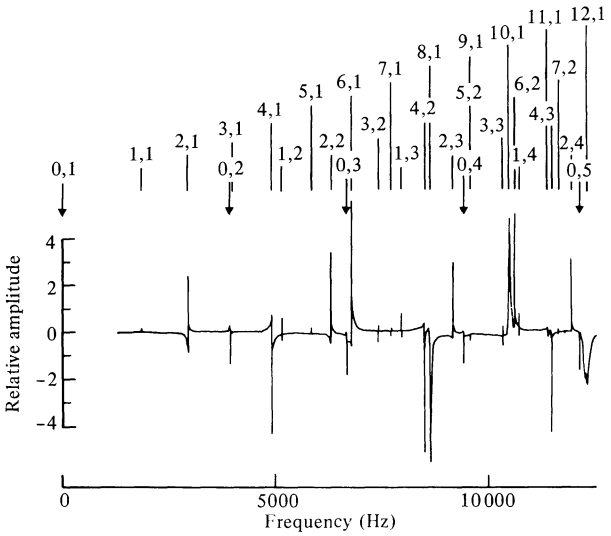

Figure 1. Top: Order and relative spacing of modes in a spherical resonator. Purely radial modes are denoted by arrows. Bottom: Measured response of a 12·7 cm diameter resonator filled with ambient air (response is at an arbitrary phase with respect to excitation). Exciting and detecting transducers are approximately point sources on the resonator wall, but 90° apart.

3 Experimental techniques

In this section we will describe the progress we have made in adapting spherical resonators in various configurations to practical problems in metrology. This is a report of continuing work; therefore we expect many of the unresolved questions raised in this section to be answered by future experiments.

All of our quantitative measurements were made with a single spherical resonator made from aluminum alloy 2024. The resonator was made in two halves which fit together with an interlocking step as sketched in figure 2. These halves were machined from cylindrical stock with a numerically controlled milling machine. When the halves were bolted together, the step insured that they were concentric. The halves were in contact only on the inner surface of the step. The aluminum shell is 1·21 cm thick and has an inside diameter of 12·700 cm. The sphere had four holes drilled through it. Two holes (3·5 mm diameter) 90° apart, as shown in figure 2, were used to introduce various sound transducers; two other holes (1·6 mm diameter) were used to couple microwave signals into and out of the resonator. These holes also allowed the gas under study to flow freely into and out of the resonator.

The resonator was not sealed. Instead, it was supported within a larger heavy-walled cylindrical container which served as both a thermostat and a pressure vessel. This aluminum cylinder was insulated from an outer aluminum cylinder which also was thermostated. The outer cylinder was held within ±0·02 K of a set temperature by circulating fluid from a commercially manufactured thermostat-circulator. The temperature of the inner thermostat was regulated at about $\frac{1}{3}$ K above that of the outer thermostat. The control point on the inner cylinder was held at a constant temperature (±0·0005 K) for several days. A differential thermopile on the outer surface of the inner thermostat indicated the top of this thermostat was consistently 0·002 K cooler than the bottom. A capsule platinum thermometer recently calibrated on IPTS-68 was thermally anchored to the resonator support inside this thermostat.

We made three independent measurements of the average diameter of the resonator. Two measurements were mechanical in nature. They involved many measurements of the coordinates in space at which a probe contacted the interior surfaces of the hemispheres. These measurements were used to estimate radii for each half. Then the distances from the steps to the bottom of the hemispheres were measured. The resulting effective diameters (the diameter of a perfect sphere with the same volume as that enclosed by the aluminum shells) from these two measurements were 12·6985 cm and 12·6954 cm. The third measurement of the average sphere

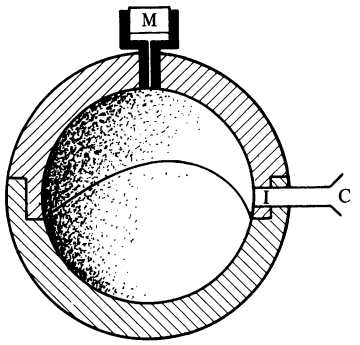

Figure 2. Sketch of resonator. Capacitor microphone probes are inserted as shown at C. Ceramic microphones are used with an adapter as shown at M.

diameter was obtained from measurements of the six lowest microwave resonances within the cavity. These resonances fall in the range 2·0–4·6 GHz and have Qs which range from 17000–35000. The observed Qs were scattered within 30% of those calculated from the DC resistivity of the aluminum alloy. Small corrections were applied to the measured frequencies for the dielectric constant of air and for the finite Qs of the resonances. The diameter of the spherical volume which would yield these frequencies is 12·6987 ± 0·0010 cm. These microwave resonances are not spherically symmetric; hence they are more sensitive to details of the resonator construction than are the radial acoustic modes.

Our best estimate for the effective diameter of the resonator is 12·6975 cm with an uncertainty of about 0·0025 cm or 2 parts in 10^4. This uncertainty is by far the largest one in our measurements of the velocity of sound. In the future, we will greatly reduce this uncertainty by first weighing the resonator in air and then weighing it when it is filled with a fluid of known density.

We experimented with four different schemes for exciting the resonator: (i) small home-made transducers hung in the center of the resonator; (ii) commercial transducers coupled to a small tube leading to the center of the resonator; (iii) commercial capacitor microphones mounted (see figure 2) in the resonator wall so that the capacitor was flush with the inner surface of the resonator; and (iv) commercial ceramic microphones mounted (see figure 2) just outside the resonator. In this last case, tightly fitting adapters were used to fill most of the coupling holes. They ended flush with the inner surface of the resonator. The first two schemes have the advantage of exciting primarily the radial modes in an efficient way. With them, high-order radial resonances may be detected by another transducer at the resonator wall with very high signal-to-noise ratios. A version of scheme (ii) was used by Bancroft (1956) to overcome the interference he encountered between the lowest radial mode (0, 2) and the nearby nonradial mode (3, 1). Unfortunately, both these schemes require corrections to the resonant frequencies which we have found hard to estimate. Thus, although these schemes may be quite valuable for relative velocity-of-sound measurements, they may introduce systematic errors into absolute measurements.

To implement the third scheme, we excited one capacitance microphone with a sinusoidal voltage of about 100 V rms. Because the microphone is a 'square-law' device and because we did not use the customary DC bias voltage, the sound generated is at twice the excitation frequency. We detected this sound with a second capacitance microphone used in the conventional manner with its own built in preamplifier. This approach has several practical advantages. Electric crosstalk between the transmitter and the receiver is not a problem since they are operating at different frequencies. Conventional, commercially available, lock-in amplifiers may be used to measure both the amplitude and the phase of the resonator response. The very wide, flat frequency resonse of the microphones does not 'pull' the cavity resonances. The capacitor microphones were placed so that the rigid back plate of the capacitor was flush with the inside wall of the resonator (see figure 2). This back plate has a high acoustic impedance as does the resonator wall itself, hence it should not change the resonator characteristics significantly.

The small commercial capacitor microphones do have some limitations which prevent us from using them under a wide range of conditions. They are rather delicate, expensive, and are limited in their tolerance for temperature extremes. They also require a preamplifier to be located right at the microphone. Thus we were led to try scheme (iv). Here we used larger (2·4 cm diameter) piezoelectric ceramic microphones. These microphones are rugged and generate a very large signal. We used adapters with these microphones in the configuration denoted by M in figure 2.

Small holes in the adapters (0·6 mm diameter) were used to conduct sound into and out of the resonator. Much smaller holes could have been used. It also would have been possible to locate these transducers much further from the sphere. This flexibility might be quite valuable, for example, in the study of gases at high temperatures.

The third transducer scheme described above was used to obtain the 'spectrum' shown in figure 1. This spectrum was obtained with the resonator sitting on a table top in the laboratory air (approximately 22 °C, 60% relative humidity). A voltage-controlled oscillator was used to sweep the drive frequency from 0 to 10 kHz in 20 min. The response of the detector was amplified, phase detected at twice the drive frequency, and displayed on an x–y recorder. The lowest 26 modes of the sphere are identified on figure 1. All these modes except the (9, 1) and (5, 2) are clearly resolved. Most importantly, the lowest radial modes are resolved (the radial modes are indicated with arrows on figure 1). In order to emphasize this point, we show in figure 3 an expanded view of the resonator response near the (0, 2) and the (3, 1) modes. The lower two curves in the figure represent the components of the output of the detecting transducer which are in phase with, and in quadrature with, the driving voltage.

The signal near the (0, 2) mode is much larger than the signal near the (3, 1) mode even though the latter is excited much more efficiently by our 'point source' transducer at the cavity wall. This is a consequence of the fact that we have chosen to place the detecting transducer 90° away from the exciting transducer, where the (3, 1) mode has a node.

To date our quantitative studies of the spherical resonator have been confined to argon. We have used the fourth transducer scheme exclusively. The argon, used as supplied, is purported to be 99·9999% pure.

In order to make precise measurements, data such as those shown in figure 3 were taken digitally. The in-phase and quadrature signals were measured with a digital voltmeter while the frequency was scanned with a synthesizer in steps of 0·1, 0·2, or 0·5 Hz in the vicinity of the resonance of interest. The measured voltages, V,

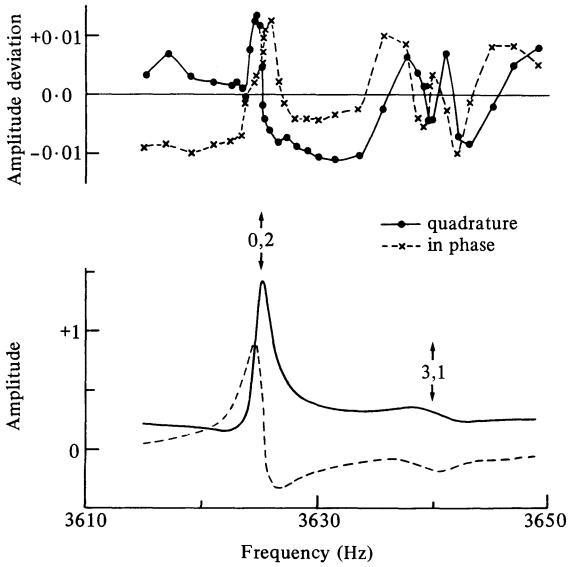

Figure 3. Bottom: In-phase and quadrature components of detector voltage as a function of excitation frequency (argon near NTP). Top: Deviations of bottom curves from fitted function.

were made to fit functions of the angular frequency, ω, of the form:

$$V = \tilde{A}\frac{\omega}{\omega_0^2 - \omega^2} + \tilde{B}\,. \tag{9}$$

Here V, $\tilde{A}$, and $\tilde{B}$ all have two components, one associated with the response of the cavity in phase with the driving voltage and one associated with the response in quadrature to the driving voltage. The complex constant $\tilde{B}$ includes a contribution to the lock-in output from electric crosstalk as well as a contribution from the acoustic response of the cavity associated with resonances far from the one or two of interest. The curves on the upper part of figure 3 show the residuals that remain after the data in the lower part of the figure are fitted to a (complex) sum of two resonances plus an additive constant. The deviations are about 1% of the original signal and are primarily a consequence of the imperfect (and drifting) orthogonality of the two channels of the lock-in.

In general, we restricted our data to within four or so line widths of the radial resonances and fitted each of them to a single resonance. For the (0, 3) and (0, 4) resonances we added a complex constant exactly as in equation (9). To describe the data near the (0, 4), (0, 5), and (0, 6) modes adequately we found it necessary to make $\tilde{B}$ in equation (9) a linear function of frequency.

Because all the resonances we used had high Qs (2200–6100), it is a satisfactory approximation to take the real part of ω_0 as the resonance frequency and the ratio of the real part of ω_0 to twice the imaginary part of ω_0 as the measured Q.

The measured resonance frequencies were divided by the factor $1-(2Q_w)^{-1}$, where Q_w was computed from the thermal conductivity of argon as calculated by Kestin et al (1972) and confirmed by the direct measurements of Guildner (1975). A further small correction (5 to 31 parts in 10^6), which is proportional to the gas density, was made for the shift in the resonance frequency arising from the finite mechanical admittance of the resonator walls. We have not yet verified that the spherical shell does indeed vibrate as we have modeled it. It is important to examine this in light of the anomalous attenuation we have encountered (see below) and in light of the importance of this correction at higher gas densities. It should be possible to measure the vibrations of the resonator walls with the aid of accelerometers.

From each corrected measurement of a resonance frequency $f_{0\ell}$ we calculated the square of the velocity of sound, $c^2 = (2a\pi f_{0\ell}/\alpha_{0\ell})^2$. Here $\alpha_{0\ell}$ is the (0, ℓ) root of equation (1). These values of c^2 are discussed in the next section.

4 Results

We have measured the velocity of sound in argon at 25·444 ± 0·002 °C and at pressures from 0·11 MPa to 0·44 MPa and at five frequencies ranging from 3·6 to 13·9 kHz. All the data taken under these conditions may be described by a linear function of pressure:

$$c^2 = c_0^2 + A_1 P\,. \tag{10}$$

We find $c_0^2 = 103589{\cdot}7$ m^2 s^{-2} with a precision of ±1·6 m^2 s^{-2} (standard deviation). This value is remarkably close to the value $\gamma RT/M = 103579$ m^2 s^{-2} for argon at 298·594 K when γ is taken to be $\frac{5}{3}$. The absolute accuracy of our measurement of c_0 is expected to be identical with the absolute accuracy with which we know the average sphere diameter (2 parts in 10^4). Thus the absolute accuracy of c_0^2 is expected to be 4 parts in 10^4. Our measurement falls well within this range. This remains true even if the data are fitted with a quadratic function of P.

In figure 4 we have displayed the deviations between the measured values of c^2 and the linear function of pressure, equation (10). It is important to note that the deviations do not depend systematically on the frequency of the sound used. This is an important confirmation of the applicability of our model for the resonator to the actual laboratory instrument. In separate experiments we verified that the resonance frequencies were independent of the amplitude of excitation.

The coefficient A_1 in equation (10) is, in the limit of zero frequency, equal to a known function of B, the second virial coefficient which occurs in the density expansion of the equation of state. This function is:

$$A_1 = \frac{2\gamma}{M}\left(B+\frac{2}{3}T\frac{dB}{dT}+\frac{2}{15}T^2\frac{d^2B}{dT^2}\right). \tag{11}$$

Our value for A_1 is $4{\cdot}60 \pm 0{\cdot}05$ m^2 s^{-2} MPa^{-1}, where the error quoted is a standard deviation from a least-squares fit. This value for A_1 agrees remarkably well with the range of values from $4{\cdot}8$ to $5{\cdot}4$ m^2 s^{-2} MPa^{-1} obtained by Rowlinson and Tildesley (1977) from an analysis of data from a variety of nonacoustic sources. They obtained values of A_1 from other thermodynamic data and independently from the interatomic potential of argon atoms (knowledge of the potential comes from transport properties and optical spectra of argon dimers).

The primary errors in our measurement of A_1 are systematic. One source which can be estimated is the contamination of this 'second acoustic virial coefficient' measurement by the third acoustic virial coefficient. We have estimated the third acoustic virial coefficient, A_2, of argon to be $0{\cdot}5$ m^2 s^{-2} MPa^{-2} from the precise velocity of sound measurements of El-Hakeem (1963) which extend from 1 to 70 atm. If we tentatively adopt this value, $A_2 = 0{\cdot}5$ m^2 s^{-2} Pa^{-2} and refit our measurements of c^2 versus P to the function

$$c^2 - 0{\cdot}5P^2 = c_0^2 + A_1P, \tag{12}$$

we find that A_1 decreases from $4{\cdot}6$ to $4{\cdot}3$ m^2 s^{-2} Pa^{-1}. Perhaps this change is a reasonable estimate of the systematic errors in A_1. Of course, we could have

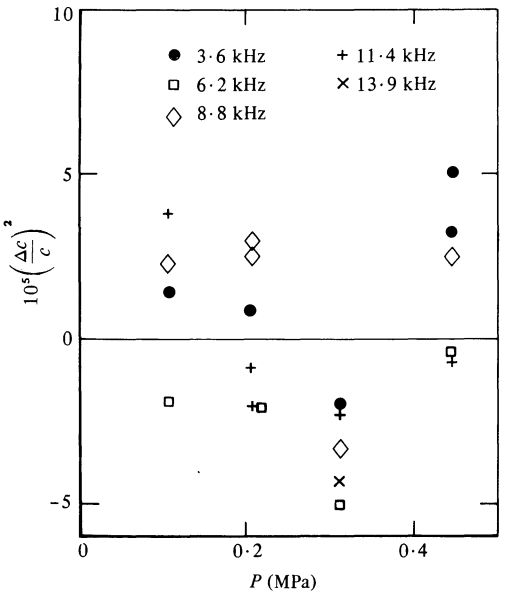

Figure 4. Fractional deviations of the square of the measured velocity of sound from a linear function of pressure (argon, 25·443 °C).

attempted to determine both A_1 and A_2 from our own data; however, it is well known that the extraction of accurate virial coefficients from equation-of-state data is a subtle problem requiring data over a wide range of pressure. We have here a correspondingly subtle problem. At the present time we choose not to commit ourselves to a best estimate of A_1, because we expect to make more extensive measurements in the near future to clarify the situation. Nevertheless we would like to remark that this change, $0{\cdot}3\ m^2\ s^{-2}\ Pa^{-1}$, in A_1 corresponds to a change of only $0{\cdot}36\ cm^3\ mol^{-1}$ in the function of the virial coefficient in the brackets in equation (11). Thus we are indeed making accurate measurements of thermophysical properties by an acoustic experiment.

We now comment briefly on the losses in the resonator and their application to transport property measurements. In the course of extracting the velocity of sound from data such as those shown in figure 3 we inevitably measure the Q of the resonances. If the model of our resonator truly reflected the behaviour of the laboratory instrument, the quantity Q^{-1}_{residual} defined in equation (8) would be zero. Furthermore, an accurate value of the thermal diffusivity could be determined from the measured Q. (Q_w is proportional to $f^{1/2}$ while Q_c is proportional to f^{-1}. This frequency dependence allows a clear separation of the two. Under our conditions Q_w/Q_c varies from 5 to 60; thus Q_w, which is proportional to $D_t^{1/2}$, dominates.) In fact, the measured Q does approach the calculated Q in some cases. This is illustrated in figure 5 where we have displayed the values obtained for $10^4 Q^{-1}_{\text{residual}}$ as a function of pressure at various frequencies. The (0, 2) resonance has a very consistent small residual loss whose average value corresponds to $Q_{\text{residual}} = 89000 \pm 18000$. This is indeed a small fraction (0·03–0·04) of the measured loss. Thus it appears that it would indeed be possible to obtain D_t from such data. On the other hand, it is also clear from figure 5 that near 8·8 kHz there are anomalously high losses in our resonator. At this frequency the residual, or unexplained, loss corresponds to an average Q_{residual} of 10000 or nearly one-third of the total loss!

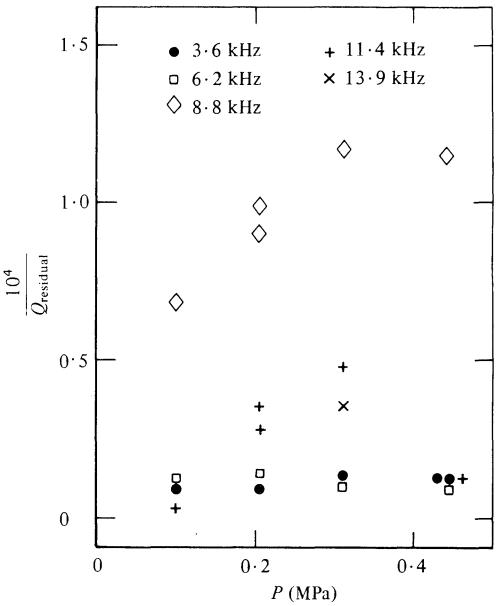

Figure 5. Q_{residual} as a function of pressure at various frequencies. Note the large residual loss near 8·8 kHz. The average Q_{residual} at 3·6 kHz is 89000. The average Q_{residual} at 8·8 kHz is 10000.

Until we have eliminated, or at least explained, this loss we cannot claim to be making accurate measurements of D_t.

If, in fact, one can measure D_t using the radial modes, it should be possible to make at least relative measurements of D_v by measuring the losses in nonradial modes.

5 Summary

We have demonstrated that the velocity of sound and its pressure dependence can be determined with an accuracy of 0·02% in dilute gases by means of a spherical resonator. It is likely that the accuracy can be greatly improved with a relatively simple refinement in the measurement of the volume of the resonator. Because the transducers are outside the resonator and need not be moved, the present approach to accurate velocity-of-sound measurements should be applicable to very high and very low temperature conditions. It seems quite likely that the theory of the spherical resonator can be refined to obtain transport properties of gases from acoustic measurements.

Acknowledgements. H Davis, T Kane, and J Little have provided invaluable technical assistance at various stages of this project. C Von Degrift assisted with the microwave measurements. Professor I Rudnick has made numerous helpful suggestions and has provided key references. His encouragement and his confidence of the eventual success of this approach to the measurement of velocity of sound was instrumental in initiating this work.

References

Bancroft D, 1956 *Am. J. Phys.* **24** 355-357
Cataland G, Plumb H H, 1973 "Low temperature thermometry: interim report" Nat. Bur. Stand. (US) Tech. Note 765
Colclough A R, 1973 *Metrologia* **9** 75-98
El-Hakeem A S, 1963 *J. Chem. Phys.* **42** 3132-3133
Gammon B E, Douslin D R, 1976 *J. Chem. Phys.* **64** 203-218
Gammon B E, 1976 *J. Chem. Phys.* **64** 2556-2568
Gammon B E, 1979 (to be published)
Guildner L A, 1975 *J. Res. Nat. Bur. Stand.* **79A** 407-413
Kestin J, Ro S T, Wakeham W A, 1972 *J. Chem. Phys.* **56** 4119-4124
Moszkowski S A, 1955 *Phys. Rev.* **99** 803-809
Plumb H H, Cataland G, 1966 *Metrologia* **2** 127-139
Quinn T J, Colclough A R, Chandler T D R, 1976 *Philos. Trans. R. Soc. London* **283** 367-420
Rayleigh J W S, 1894 *Theory of Sound* (reprinted in 1945, New York: Dover Publications)
Rowlinson J S, Tildesley D J, 1977 *Proc. R. Soc. London* **A358** 281-286
Slater J C, 1959 *Microwave Electronics* (New York: Van Nostrand) pp 57-83